Diffuse backscattering Mueller matrices of highly scattering media

Andreas H. Hielscher, Angelia A. Eick, Judith R. Mourant, Dan Shen*, James P. Freyer*, and Irving J. Bigio

*Chemical Science and Technology Division and Life Sciences Division**
Los Alamos National Laboratory, CST-4, MS E535, Los Alamos, New Mexico 87545

hielsch@lanl.gov

Abstract: We report on the development of a method that records spatially dependent intensity patterns of polarized light that is diffusely backscattered from highly scattering media. It is demonstrated that these intensity patterns can be used to differentiate turbid media, such as polystyrene-sphere and biological-cell suspensions. Our technique employs polarized light from a He-Ne laser (λ = 543 nm), which is focused onto the surface of the scattering medium. A surface area of approximately 4x4 cm centered on the light input point is imaged through polarization-analysis optics onto a CCD camera. One can observe a large variety of intensity patterns by varying the polarization state of the incident laser light and changing the analyzer configuration to detect different polarization components of the backscattered light. Introducing the Mueller-matrix concept for diffusely backscattered light, a framework is provided to select a subset of measurements that comprehensively describe the optical properties of backscattering media.

OCIS codes: (170.1530) Cell analysis; (170.5280) Photon migration; (290.0290) Scattering; (290.1350) Backscattering; (290.4210) Multiple scattering; (290.7050) Turbid media

References

1. J.M. Schmitt, A.H. Gandjbakhche and R.F. Bonner, "Use of polarized-light to discriminate short-path photons in a multiply scattering medium," *Appl. Opt.* **31**, 6535-6546 (1992).
2. R.R. Anderson, "Polarized-light examination and photography of the skin," *Arch. Dermatol.* **127**, 1000-1005 (1991).
3. S.L. Jacques, L.H. Wang, D.V. Stephens, and M. Ostermeyer, "Polarized light transmission through skin using video reflectometry: toward optical tomography of superficial tissue layers," in *Lasers in Surgery: Advanced Characterization, Therapeutics, and Systems VI*, R. R. Anderson, ed., Proc. SPIE **2671**, pp. 199-220 (1996).
4. S.G. Demos, and R.R. Alfano, "Optical polarization imaging," *Appl. Opt.* **36**, 150-155 (1997).
5. A.H. Hielscher, J.R. Mourant, I.J. Bigio, "Diffuse polarization spectroscopy on tissue phantoms and biological cell suspensions", in *Optical Biopsies and Microscopic Techniques*, I.J. Bigio, W.S. Grundfest, H. Schneckenburger, K. Svanberg, P.M. Viallet, eds., Proc. SPIE **2926**, pp. 67-76 (1996).
6. A.H. Hielscher, J.R. Mourant, I.J. Bigio, "Influence of particle size and concentration on the diffuse backscattering of polarized light from tissue phantoms and biological cell suspensions," *Appl. Opt.* **36**, 125-135 (1997).
7. W.S. Bickel and W.M. Bailey, "Stokes vectors, Mueller matrices, and polarized light scattering," *Am. J. Phys.* **53**, 468-478 (1985).
8. H.C. van de Hulst, *Light Scattering by Small Particles* (John Wiley&Sons, New York, NY, 1957)
9. W.S. Bickel, A.J. Watkins, and G. Videen, "The light-scattering Mueller matrix elements for Rayleigh, Rayleigh-Gans, and Mie spheres," *Am. J. Phys.* **55**, 559-561 (1987).
10. L.C. Junqueira, J. Carneiro, and R.O. Kelley, *Basic Histology* (Appleton&Lange, Norwalk, Connecticut, 1992), pp. 108-110.
11. L.A. Kunz-Schugart, K. Groebe, and W. Mueller-Klieser, "Three-dimensional cell culture induces novel proliferative and metabolic alterations associated with oncogenic transformation," *Int. J. Cancer*. **66**, 578-586 (1996).
12. K.E. LaRue, E.M. Bradbury, and J.P. Freyer, "Regulation of G1 transit by cyclin kinase inhibitors in multicellular spheroid cultures of rat embryo fibroblast cells transformed to different extents," *Cancer Res.*, in press (1998).
13. S.L. Jacques, A. Gutsche, J. Schwartz, L. Wang, and F.K. Tittel, "Video reflectometry to extract optical properties of tissue in vivo," in *Medical Optical Tomography: Functional Imaging and Monitoring*, G. Mueller, B. Chance, R.R. Alfano, S.R. Arridge, J. Beuthan, E. Gratton, M. Kaschke, B.R. Masters, S.

#2826 - $10.00 US Received October 8, 1997; Revised December 2, 1997

Svanberg, and P. van der Zee, eds., Vol. ISII of SPIE Institute Series (Society of Photo-Optical Instrumentation Engineers, Bellingham, WA, 1992) pp. 211-226.
14. A. Kienle, L. Lilge, M.S. Patterson, R. Hibst, R. Steiner, and B.C. Wilson, "Spatially resolved absolute diffuse reflectance measurements for noninvasive determination of the optical scattering and absorption coefficients of biological tissue," *Appl. Opt.* **35**, 2304-2314 (1996).
15. T.J. Farrell, M.S. Patterson, and B. Wilson, "A diffusion theory model of spatially resolved, steady-state diffuse reflectance for the noninvasive determination of tissue optical properties in vivo," *Med. Phys.* **19**, 879-888 (1992).
16. J.R. Mourant, T. Fuselier, J. Boyer, T.M.. Johnsons, and I.J. Bigio, "Predictions and measurements of scattering and absorption over broad wavelength ranges in tissue phantoms," *Appl. Opt.* **36**, 949-957 (1997).
17. M.G. Nichols, E.L. Hull, and T.H. Foster, "Design and testing of a white-light, steady-state diffuse reflectance spectrometer for determination of optical properties of highly scattering systems," *Appl. Opt.* **36**, 93-104 (1997).
18. J.T. Bruulsema, J.E. Hayward, T.J. Farrel, M.S. Patterson, L. Heinemann, M. Berger, T. Koschinsky, J. Sandahlchristiansen, and H. Orskov, "Correlation between blood-glucose concentration in diabetics and noninvasively measured tissue optical scattering coefficients," *Opt. Lett.* **22**, 190-192 (1997).
19. A. Kienle and M.S. Patterson, "Improved solutions of the steady-state and time-resolved diffusion equation for reflectance from a semi-infinite turbid medium," *J. Opt. Soc. of Am. A* **14**, 246-254 (1997).
20. R. Bays, G. Wagnieres, D. Robert, D. Braichotte, J.F. Savary, P. Monnier, and H. Vandenbergh, "Clinical determination of tissue optical properties by endoscopic spatially-resolved reflectometry," *Appl. Opt.* **35**, 1756-1766 (1996).
21. H.L. Liu, D.A. Boas, Y.T Zhang, A.G. Yodh, and B. Chance, "Determination of optical-properties and blood oxygenation in tissue using continous NIR light," *Phys. Med. Biol.* **40**, 1983-1993 (1995).
22. P. Marquet, F. Bevilacqua, C. Depeursinge, E.B. Dehaller, "Determination of reduced scattering and absorption coefficients by a single charged coupled device array measurement: 1. Comparison between experiments and simulations," *Opt. Eng.* **34**, 2055-2063 (1995).
23. L.H. Wang and S.L. Jaques, "Hybrid model of Monte Carlo simulations and diffusion theory for light flectance by turbid media," *J. Opt. Soc. Am. A* **10**, 1746-1752 (1993).
24. T.J. Farrell, B.C. Wilson, and M.S. Patterson, "The use of a neural network to determine tissue optical properties from spatially resolved diffuse reflectance mesurements.," *Phys. Med. Biol.* **37**, 2281-2286 (1992).

1. Introduction

In recent years there has been an increased interest in the propagation of polarized light in highly scattering media, especially biological materials. For example, Schmitt et al [1] proposed to use transmitted polarized light for imaging tissue heterogeneities. Anderson et al [2] Jacques et al [3] and Demos et al [4] studied the use of backreflected polarized light for surface and beneath-the-surface imaging. Furthermore, our group previously demonstrated that diffusely backscattered, linearly polarized light can be used to determine the scattering coefficient, μ_s, anisotropy factor, g, and average particle size of polystyrene-sphere and biological-cell suspensions. [5,6]

In this work, we generalize our studies of diffusely backscattered polarized light from highly scattering media by including measurements of circularly polarized light and introducing the Mueller-matrix concept. While the Mueller matrix is well known to describe many optical elements and materials, [7-9] matrix elements have not been obtained for diffusely backscattered light from turbid media. We will show matrix elements for various polystyrene-sphere suspensions, and for cancerous and noncancerous cell suspensions. In particular it is demonstrated that cancerous rat fibroblast cells, MR1, can best be distinguished from noncancerous cells, M1, by measuring backreflected circularly polarized light.

2. Methods

2.1 Experimental setup

The experimental setup for studying the diffuse backreflectance of polarized light is depicted in Fig. 1. A He-Ne laser with an output power of 5 mW at a wavelength of λ = 543 nm is used as the light source. Polarization optics P1 are placed in front of the HeNe laser. To generate linearly polarized light at various angles a dichroic sheet polarizer (Melles Griot) is mounted onto a rotation stage. Circularly polarized light is generated, by inserting a $\lambda/4$ mica retardation plate (Melles Griot) behind the linear polarizer, with the retarder principal plane at $\pm 45^{o}$ with respect to the electrical field vector of the incident linearly polarized beam. The polarized light is focused to a spot with a diameter d < 500 μm by lens L1 (f = 15 cm) via mirror M1, through a hole in the center of mirror M2, onto the surface of the scattering

#2826 - $10.00 US Received October 8, 1997; Revised December 2, 1997

medium. The beam is perpendicular to the surface of the medium. Lens L2 (f = 15 cm) is used to generate an image of the surface-area around the input point at the image plane IP1. This intermediate image plane allows us to place an optical mask (diameter = 2 mm) in the center of this image. In this way the strong specular reflection from the surface at the laser input point is rejected, and only multiply scattered light is recorded. The image at IP1 including the optical mask was viewed with a 55-mm Nikon camera lens L3 (Micro-Nikkor, 55 mm, f/2.8), which was mounted on a cooled CCD camera (Princeton Instrument, Inc.). The CCD chip has 575x384 pixels with a pixel size of 20x20 μm. The surface-area under observation around the laser entrance point could be varied from 0.5x0.5 cm to 4x4 cm, depending on the position of L2 and L3. A polarizer P2 was placed in front of L3 to serve as an analyzer. The CCD camera was controlled and operated with IPLab software (Signal Analytics Cooperation). The dynamic range of the CCD camera was 14 bits. Two typical examples of images obtained with this set-up are shown in Fig. 2.

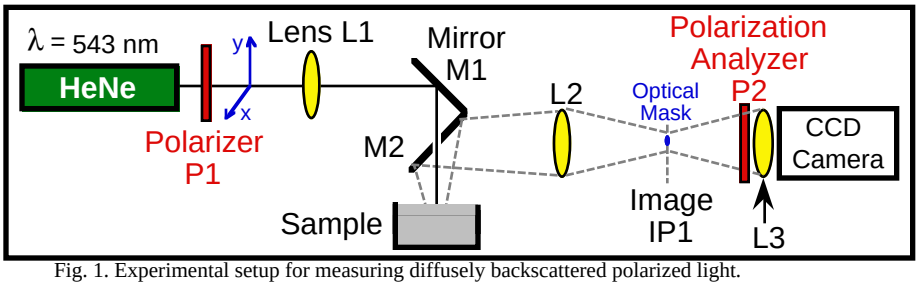

Fig. 1. Experimental setup for measuring diffusely backscattered polarized light.

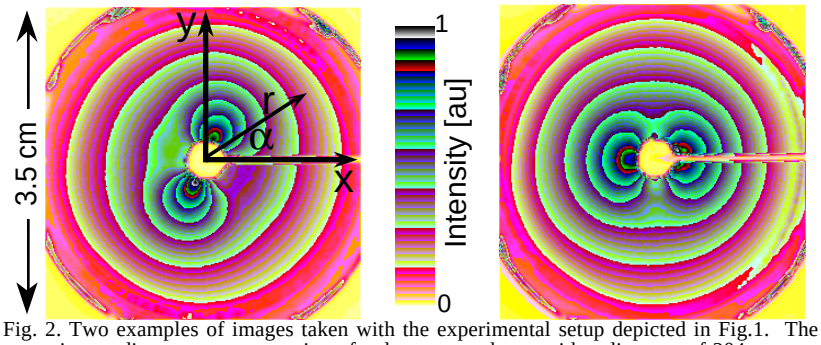

Fig. 2. Two examples of images taken with the experimental setup depicted in Fig.1. The scattering medium was a suspension of polystyrene-spheres with a diameter of 204 nm at a concentration of 0.05% by weight. Using Mie-theory[8] the scattering coefficient of the suspension was calculated to be $\mu_s' = 1.9\ cm^{-1}$. In Fig. 2a (left) the incident beam was linearly polarized at +45° with respect to the x-axis and the analyzer consisted of a linear polarizer oriented along the y-axis. Fig. 2b (right) was obtained with a right-hand circularly polarized incident beam and the linear polarization analyzer oriented along x-axis. The line that enters the images from the right is caused by the needle that holds the optical mask, which obscures the center of the images. To better illustrate the azimuthal dependence of the intensity decay the images are shown in a false-color depiction. The yellow areas in the corner of the images are outside the cylindrical beaker that contains the particle suspensions.

2.2 Materials

We prepared four different types of aqueous, monodisperse polystyrene-sphere suspensions. The spheres had diameters of 204 nm, 497 nm, 890 nm, 2040 nm and were suspended in deionized water with trace amounts of surfactants (Duke Scientific Corporation, 2463 Faber Place, P.O. Box 50005, Palo Alto, California 94303). We chose particle concentrations that resulted in reduced scattering coefficients, $\mu_s' = (1-g)\,\mu_s$, in the range of 1.8 to 2.2 cm^{-1}, which is comparable to values found for the cell suspensions used in this work.

To study diffuse backreflection from biological material, we prepared suspensions of cancerous (MR1) and noncancerous (M1) rat fibroblast cells. Fibroblasts are most commonly found in connective tissue and are responsible for the synthesis of fibers and amorphous intercellular substances. Fibroblasts are rich in mitochondria, lipid droplets, Golgi

#2826 - $10.00 US
Received October 8, 1997; Revised December 2, 1997

complexes, and rough endoplasmic reticulum. [10] The cells used in this study came from the same rat-embryo fibroblasts into which a mutated myc-gene is transfected to obtain M1 cells, while an additional mutant ras-gene transfection leads to MR1 cells. [11] Only MR1 cells form a tumor if injected into a rat. Cell suspensions were prepared from monolayers grown in roller bottles and suspended in ice-cold phosphate-buffered salineat a concentration of 10^8 cells/cm^3. [6,12] Approximately 30 ml of each suspension was used for the backscattering experiments. To obtain the backscattered intensity images, the suspensions were placed in a 4 cm diameter cylindrical beaker, with a suspension depth of approximately 2.5 cm.

2.3 Polarization arithmetic for diffusely backscattered light

A large number of different experiments are possible if one wants to study the polarization-dependent scattering properties of turbid media. The probing light may be linearly polarized at various angles, right-hand circularly, left-hand circularly, or elliptically polarized. Light coming from the scattering medium can be analyzed in the same numerous ways. However, only a few measurements are needed to completely characterize the optical properties of any material. The necessary procedure is elegantly demonstrated by the Stokes-vector Mueller-matrix approach to polarization and light scattering. [7]

2.3.1 Stokes vector

Each light beam can be represented by its four-component Stokes vector, S = (I,Q,U,V). The components of the Stokes vector are related to the electric field vectors as follows:

$$S = \begin{bmatrix} I \\ Q \\ U \\ V \end{bmatrix} = \begin{bmatrix} \langle E_h E_h^* + E_v E_v^* \rangle \\ \langle E_h E_h^* - E_v E_v^* \rangle \\ \langle E_h E_v^* + E_v E_h^* \rangle \\ \langle i(E_h E_v^* - E_v E_h^*) \rangle \end{bmatrix} \tag{1}$$

where E_h and E_v are electric field components horizontal and vertical with respect to the direction of light travel. The "*" indicates the complex conjugate, and the brackets represent time averages over time periods longer than T = 1/f, where f is the optical frequency (~10^{15}/s). Some of the Stokes components have an obvious interpretation. For example, $I = \langle E_h E_h^* + E_v E_v^* \rangle$ is the time average of the sum of the products of the E-field amplitudes, which is equal to the total intensity. Examples for the Stokes vector notation are, unpolarized light: [1,0,0,0], horizontal linearly polarized light: [1,1,0,0], vertical linearly polarized light: [1,-1,0,0], right-hand circular polarized light: [1,0,0,1], and left-hand circular polarized light: [1,0,0,-1].

2.3.2 Mueller matrix

In general, the interaction of light with optical elements such as lenses, polarizers, filters, surfaces, scattering media etc., changes the polarization state of the light from S to S'. When light is described by a four-component vector, this interaction with any optical element or material can be described as a multiplication of the Stokes vector with a 4x4 matrix, S' = M S. This sixteen-element matrix is called the Mueller matrix or, if scattering is involved, the scattering matrix:

$$M = \begin{bmatrix} M_{11} & M_{12} & M_{13} & M_{14} \\ M_{21} & M_{22} & M_{23} & M_{24} \\ M_{31} & M_{32} & M_{33} & M_{34} \\ M_{41} & M_{42} & M_{43} & M_{44} \end{bmatrix} \tag{2}$$

This matrix completely characterizes any component or material in terms of its optical properties. For example, a linear polarizer is described by $M_{11} = M_{12} = M_{21} = M_{22} = 1$ and all other elements equal to zero. A right-hand circular polarizer is represented by $M_{11} = M_{14} = M_{41} = M_{44} = 1$, and all other elements equal to zero.

#2826 - $10.00 US Received October 8, 1997; Revised December 2, 1997

In this work we consider diffusely backscattered light from turbid media. We photograph the surface around the laser input point (see Figs. 1 and 2). Therefore, rather than being just one number, each of the sixteen elements of the scattering matrix is a 2D array of numbers referring to different spatial locations on the surface of the medium. An example is shown in the next section.

2.3.3 Determining the Mueller matrix

If the Mueller matrix is not known, all the elements can be determined experimentally. It can be shown that 49 intensity measurements with various orientations of polarizers and analyzers are necessary to obtain the 16 elements of the Mueller matrix. [7] Figure 3 lists the necessary measurements for each matrix element. For example, to obtain the M_{11} element one needs to

M11: (OO)	**M12:** (HO-VO)/2	**M13:** (PO-MO)/2	**M14:** (LO-RO)/2
M21: (OH-OV)/2	**M22:** (HH+VV)/4 – (HV+VH)/4	**M23:** (PH+MV)/4 – (PV+MH)/4	**M24:** (LH+RV)/4 – (LV+RH)/4
M31: (OP-OM)/2	**M32:** (HP+VM)/4 – (HM+VP)/4	**M33:** (PP+MM)/4 – (PM+MP)/4	**M34:** (LP+RM)/4 – (LM+RP)/4
M41: (OL-OR)/2	**M42:** (HL+VR)/4 – (HR+VL)/4	**M43:** (PL+MR)/4 – (PR+ML)/4	**M44:** (LL+RR)/4 – (RL+LR)/4

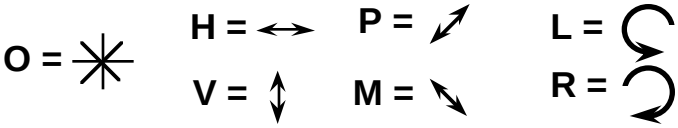

Fig. 3. This chart shows how to measure the various Mueller matrix elements. A two letter combination stands for one measurement. For example the combination (HV) means that the incoming light is linearly polarized along the horizontal axis (x-axis, see Fig. 2) and the analyzer is set to transmit light that is linearly polarized along the vertical axis (y-axis). For example, to calculate M_{22} four measurements are necessary: (HH), (VV), (HV) and (VH).

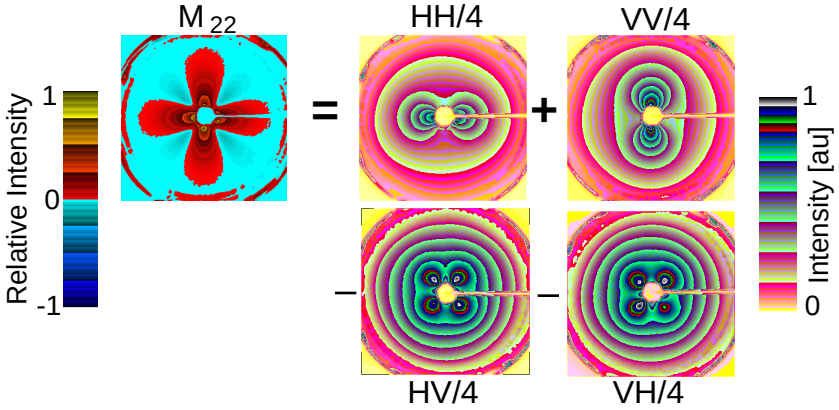

Fig. 4. Calculation of the Matrix element M_{22} from images obtained for the same polystyrene-sphere suspensions as shown in Fig. 2. Note that the color codes are different for the two sides of the equation, to allow for negative values of the matrix elementt.

#2826 - $10.00 US Received October 8, 1997; Revised December 2, 1997

measure the total reflected intensity from an unpolarized incident beam. The M_{12} element is obtained by measuring the total reflected intensity for a horizontally, linearly polarized incoming beam and subtracting from this the total reflected intensity for a vertically, linearly polarized incoming beam. Fig. 4 graphically depicts the calculation of the M_{22} element.

Once all 16 elements of the matrix are obtained, the medium is completely described in terms of its optical characteristics. In our case this means: Given any state of polarization of the incident beam it is possible to calculate the state of polarization (Stokes vector) of the diffusely backscattered light. For example if the incident beam is linearly polarized along the x-axes, the Stokes vector is given by S = [1,1,0,0]. This vector is multiplied by the Mueller matrix, M, to calculate the Stokes vector of the diffusely backscattered light. This light encounters an analyzer consisting of a linear polarizer along the y-axis, with $M_{11} = M_{22} = 1$ and $M_{21} = M_{12} = -1$ and all other elements equal to 0. Putting it all together we obtain:

$$\begin{bmatrix} I \\ Q \\ U \\ V \end{bmatrix} = \begin{bmatrix} 1 & -1 & 0 & 0 \\ -1 & 1 & 0 & 0 \\ 0 & 0 & 0 & 0 \\ 0 & 0 & 0 & 0 \end{bmatrix} \bullet \begin{bmatrix} M_{11} & M_{12} & M_{13} & M_{14} \\ M_{21} & M_{22} & M_{23} & M_{24} \\ M_{31} & M_{32} & M_{33} & M_{34} \\ M_{41} & M_{42} & M_{43} & M_{44} \end{bmatrix} \bullet \begin{bmatrix} 1 \\ 1 \\ 0 \\ 0 \end{bmatrix} \tag{3a}$$

$$\begin{bmatrix} I \\ Q \\ U \\ V \end{bmatrix} = \begin{bmatrix} M_{11} + M_{12} - M_{21} - M_{22} \\ -M_{11} - M_{12} + M_{21} + M_{22} \\ 0 \\ 0 \end{bmatrix} \tag{3b}$$

As pointed out in section (2.3.1) the first component, I, of the Stokes vector is equal to the total intensity. This is the parameter measured with the setup shown in Fig. 1. Therefore the measured intensity will equal the sum of the four Mueller matrix elements $M_{11} + M_{12} - M_{21} - M_{22}$, of which M_{22} for a 204-nm-sphere suspension is displayed in Fig. 4.

It should be noted that the M_{11} element, which is obtained by using no polarizing optics in the setup, equals the measurements done by Jacques et al [13] and Kienle et al [14], who call this "video-reflectometry". They show that one can determine μ_s' and μ_a of the medium by analyzing the intensity decay as a function of r, the distance from the laser entry point into the medium. If M_{11} does not depend on the azimuthal angle, α (see Fig. 2a), it is possible to measure the intensity decay as a function of r in one dimension, rather than taking a two-dimensional image of the surface intensities. This method, often referred to as spatially-resolved diffuse-reflectance measurement, has been used by many authors to determine optical properties of tissue phantoms and biological tissues. [15-24]

The introduction of the Mueller-matrix concept for the diffusely backscattered light provides, in addition to the widely used M_{11} element, 15 more elements, which can be evaluated to obtain further information about scattering media. Because the description of the optical characteristics with the Mueller matrix is complete, any information about particle size, refractive index, particle shape etc. has to be found in the Mueller matrix by careful analysis of the matrix elements. If some information about the medium cannot be extracted from the various matrix elements, this information cannot be extracted from any other additional backscattering measurements. However, further information may be gained, for example, by measuring the diffuse transmittance, the diffuse backreflectance at different incident and observation angles, or time-dependent polarization effects.

Given the vast literature that deals with M_{11}-type measurements and how these can be used to determine optical properties of turbid media, it is clear that one could devote an entire study to each of the other 15 elements. Such a detailed analysis is beyond the scope of this paper. Instead we have chosen several examples that illustrate the potential of the Mueller matrix approach to characterize highly scattering media.

#2826 - $10.00 US Received October 8, 1997; Revised December 2, 1997

3. Results

3.1. Polystyrene-sphere suspensions

Figure 5 shows all 16 Mueller matrix elements obtained for a polystyrene-sphere suspension, with particles of 204-nm diameter. The particle concentration is 0.05% by weight, which results in a reduced scattering coefficient of $\mu_s' = 1.9\ cm^{-1}$. The displayed intensities are relative to the maximum intensity of the M_{11} element. This element is always positive, however, all other elements can have negative values, because different intensity measurements are subtracted from each other (See Fig. 3). Positive values are displayed in red-yellow colors, while negative values are indicated in blue tones.

We can make several observations: First we notice that $M_{nm} = M_{mn}$, which means that this Mueller matrix is symmetric. The difference between the measurement of M_{mn} and

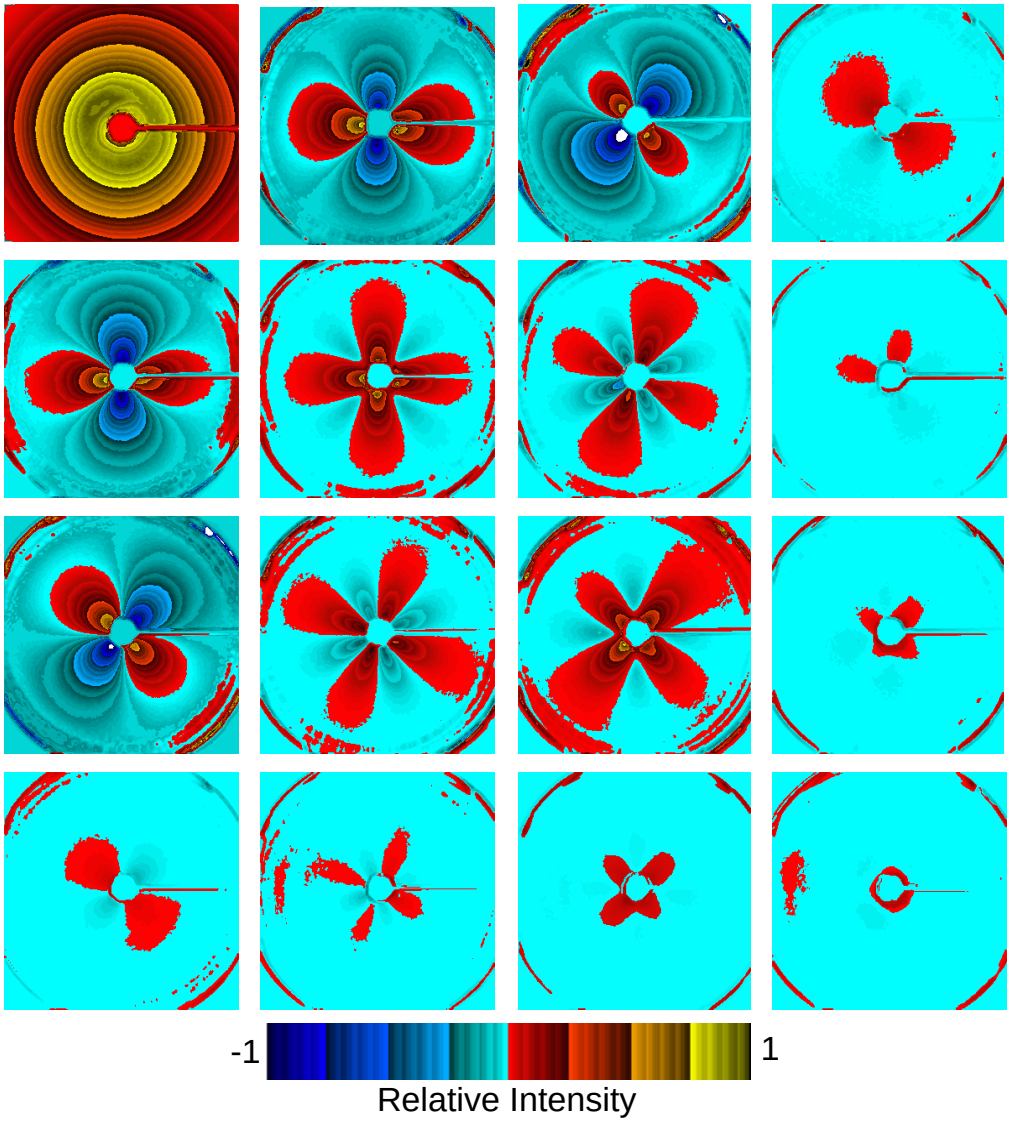

Fig. 5. Diffuse backscattering Mueller matrix elements of polystyrene-sphere suspension withmonodisperse particle diameter of d = 204 nm ($\mu_s' = 1.9\ cm^{-1}$). The upper left corner is M_{11}, the lower right corner is M_{44} (see Eq. 2 and Fig. 3). The color scale is normalized so that the maximum intensity of the M_{11} element equals 1. All images displayed are 3.5cm x 3.5cm.

#2826 - $10.00 US
Received October 8, 1997; Revised December 2, 1997

of M_{nm} is simply that the polarization optics before and after the medium are exchanged. (see. Fig. 1, optical elements P1 and P2). Therefore, if the scattering medium is not optically active and has no internal structure that results in some preferred optical axis, M_{nm} should indeed equal M_{mn}. Furthermore, several pairs of elements exist that differ only in the orientation of the intensity pattern. For example M_{13} can be obtained by rotating M_{12} by 45 degrees. The same relation holds for the pairs M_{31} and M_{21}, and M_{22} and M_{33}. The only difference between the measurements of these pairs is a rotation of the polarization and analyzer optics (P1 and P2 in Fig. 1) by 45 degrees. Again, if the suspension is not optically active and has no preferential optical direction this result should be expected. Finally, we observe that the elements in the last column (M_{14}, M_{24}, M_{34}, M_{44}) and the last row (M_{41}, M_{42}, M_{43}, M_{44}) are almost zero, while all other elements show strong azimuthal variations in the relative intensity.

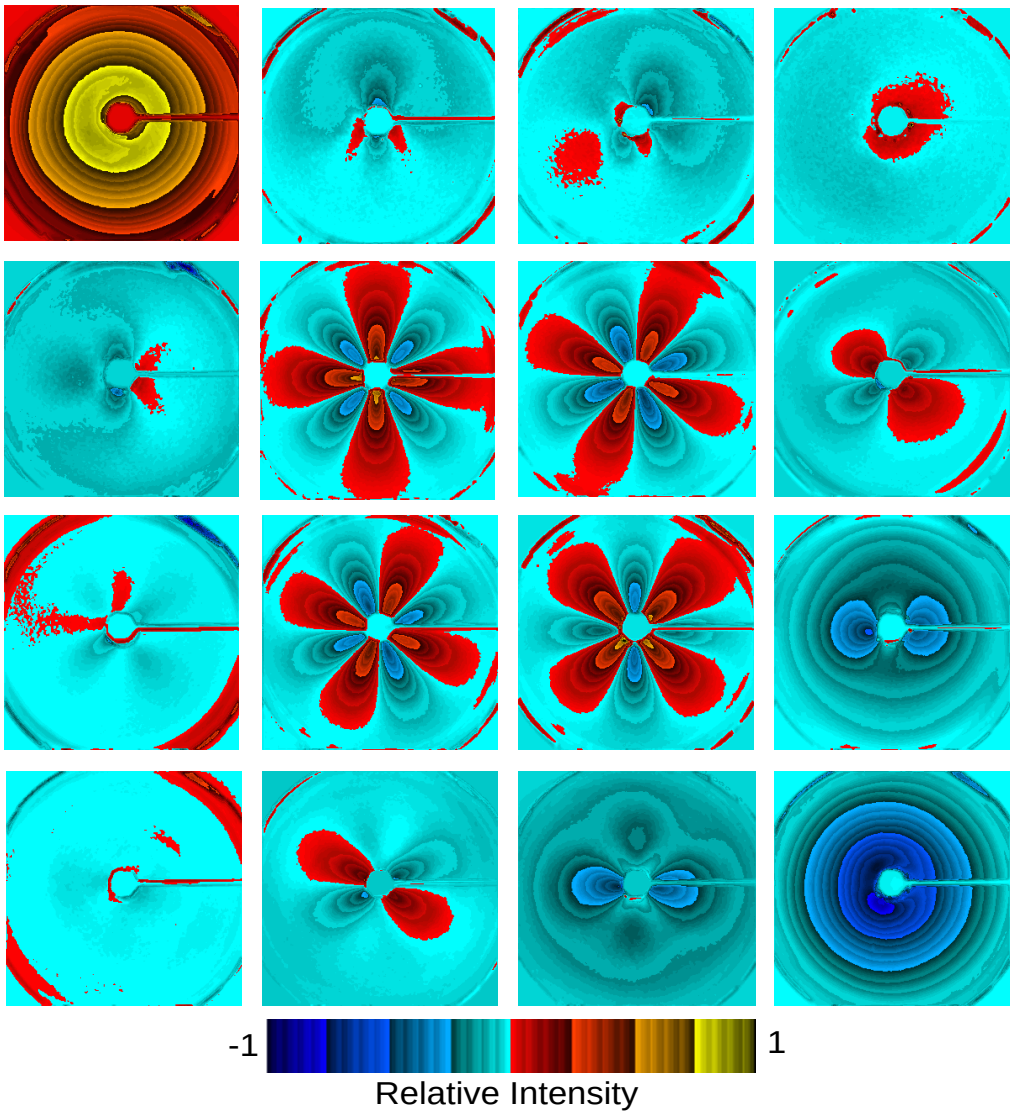

Fig. 6. Diffuse backscattering Mueller matrix elements of a polystyrene-sphere suspension with monodisperse particle diameter of d = 2040 nm (with $\mu_s' = 1.9\ cm^{-1}$). All images displayed are 3.5cm x 3.5cm.

#2826 - $10.00 US
Received October 8, 1997; Revised December 2, 1997

The last observation is especially interesting, when the 204-nm-particle suspension of Fig. 5 is compared to the suspension of 2040-nm-diameter spheres ($\mu_s' = 1.9\ cm^{-1}$) in Fig. 6. In this case the last row and last column show azimuthal intensity variations, while the first row and first column (M_{12}, M_{13}, M_{14}, and M_{21}, M_{31}, M_{41}) are almost zero. Other differences are the more pronounced azimuthal variation of the center elements M_{22}, M_{32}, M_{23}, and M_{33}. The matrix symmetries are the same as for the 204-nm sphere suspensions. Also, since the reduced scattering coefficient of the two suspensions are identical, the M_{11} elements are the same. (The radial intensity decay only depends on μ_s' and μ_a, [14] and μ_a is negligible in both cases.) This demonstrates the advantages of the Mueller matrix approach over standard video reflectometry, which is based on unpolarized light measurements. The addition of polarization properties allows to distinguish between 204-nm and 2040-nm sphere suspensions, even when the reduced scattering coefficients are the same.

All sixteen Mueller matrix components together provide a "finger print" of the scattering medium under investigation. As just shown, looking at the entire Mueller matrix often enables one to distinguish qualitatively between two media. To obtain a more quantitative distinction between different media, more detailed analyses of single matrix elements are necessary. As an example we investigated changes in the M_{44} element as a function of particle diameter in monodisperse, polystyrene-sphere suspensions.

The M_{44} element is calculated from 4 measurements, which involve only circularly polarized light (see Fig.3: $M_{44} = LL + RR - LR - RL$). This element is a measure of how effectively a medium flips the helicity of the backscattered light. For a perfect mirror the element $M_{44} = -1$, because perpendicular-incoming left-hand circularly polarized light returns right-hand circularly polarized and vice a versa. (Therefore, LL = RR = 0 and LR = RL = 1).

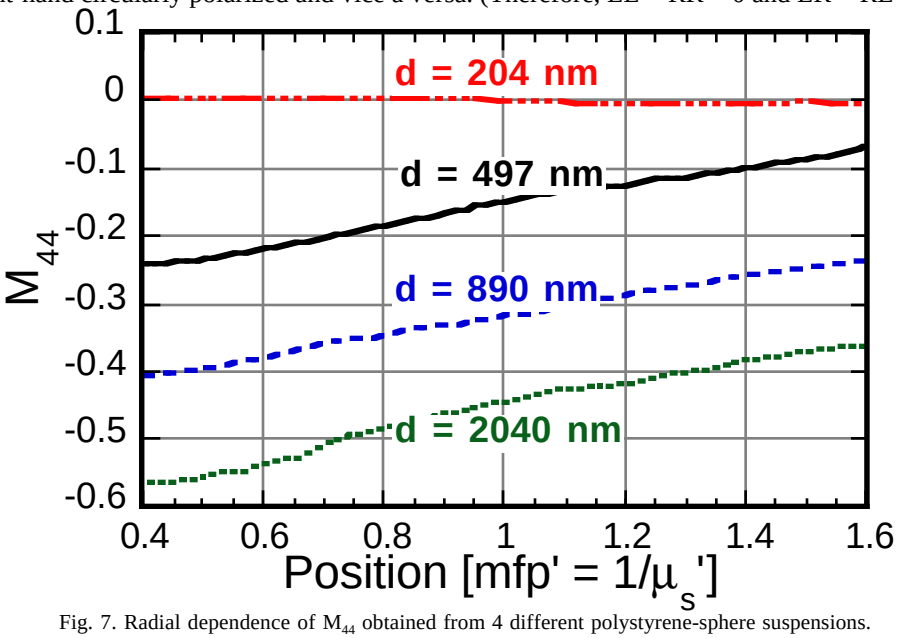

Fig. 7. Radial dependence of M_{44} obtained from 4 different polystyrene-sphere suspensions. The numbers indicate the diameter, d, of the spheres in the suspension. The radial distance is given in units of transport mean free path (mfp').

We found that in the case of polystyrene-sphere suspension, M_{44} has no azimuthal dependence. Therefore, we extracted the values of this element along the y-axes from the 2-dimensional images of M_{44}. The results for four different sphere suspensions are shown in Fig. 7. It can be seen that M_{44} decreases with increasing sphere diameter. Therefore, the suspensions with larger spheres flip the helicity more effectively, and most of the backscattered light has a different helicity than the incident light. This behavior can be understood if one considers that with increasing diameter the spheres become more and more

#2826 - $10.00 US
Received October 8, 1997; Revised December 2, 1997

like a mirror, which can be thought of as a sphere with infinite radius. If the polystyrene spheres are small (d = 204 nm) compared to the wavelength (λ = 543 nm), the backscattered light is equally left-hand and right-hand polarized and the element is zero. Furthermore, the effect is strongest in the center, near the laser entry point. Here the backscattered light has undergone only a few scattering events and the polarization effects are strongest. With increasing distance from the point of light incident, the number of scattering events increases and eventually the polarization information is lost - the value of the M_{44} approaches 0.

3.2 Cells suspensions

In addition to monodisperse particle suspensions with known optical properties, we also applied the Mueller matrix approach to biological cell suspensions. Figures 8 and 9 show the results obtained for cancerous (MR1) and noncancerous (M1) rat fibroblast suspensions. Both suspensions contain 10^8cells/cm^3 and the scattering coefficient were $\mu_s' = 2.2$ cm^{-1}(±10%)

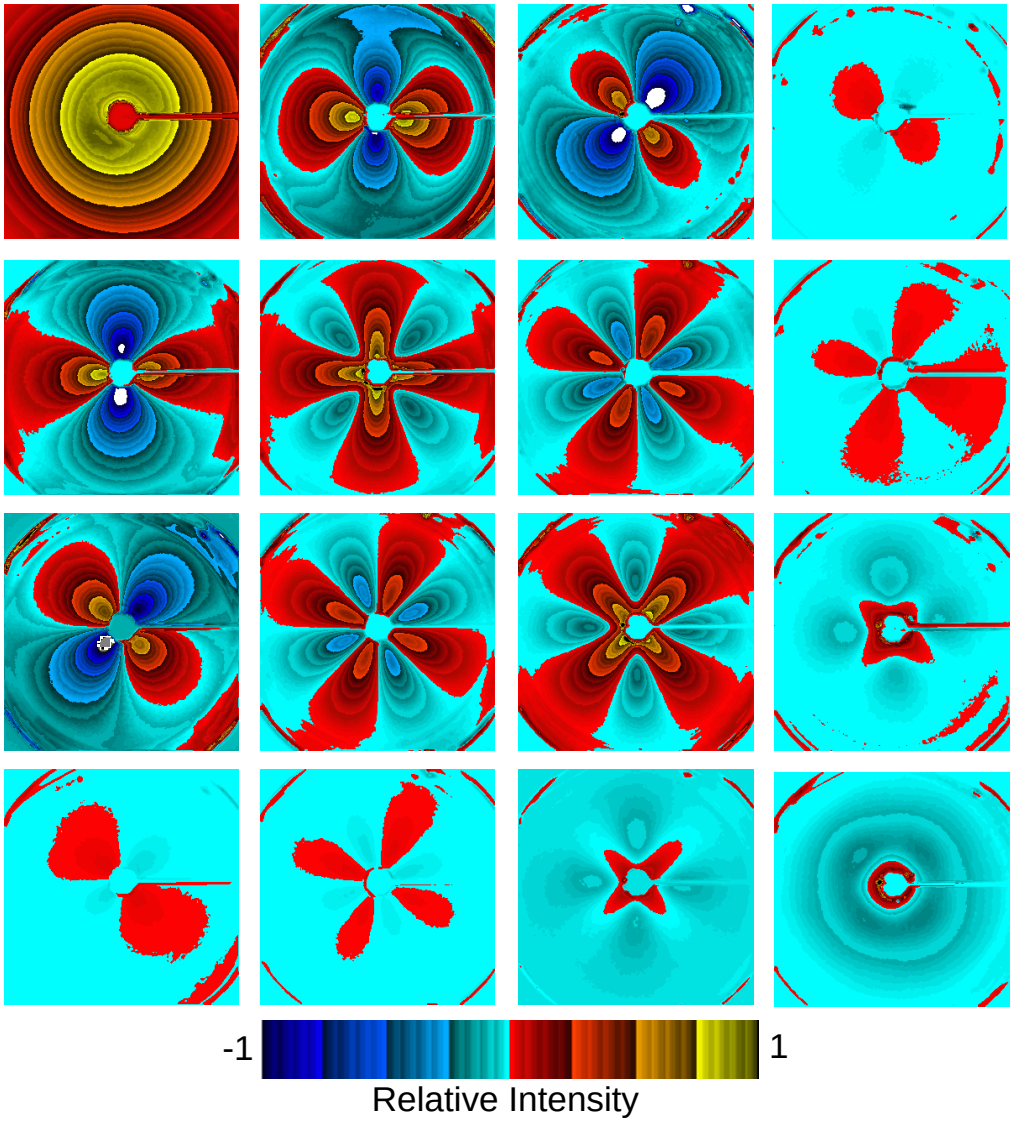

Fig.8. Diffuse-backscattering Mueller matrix of M1 cell suspension with 10^8 cells/cm^{-3}.

#2826 - $10.00 US
Received October 8, 1997; Revised December 2, 1997

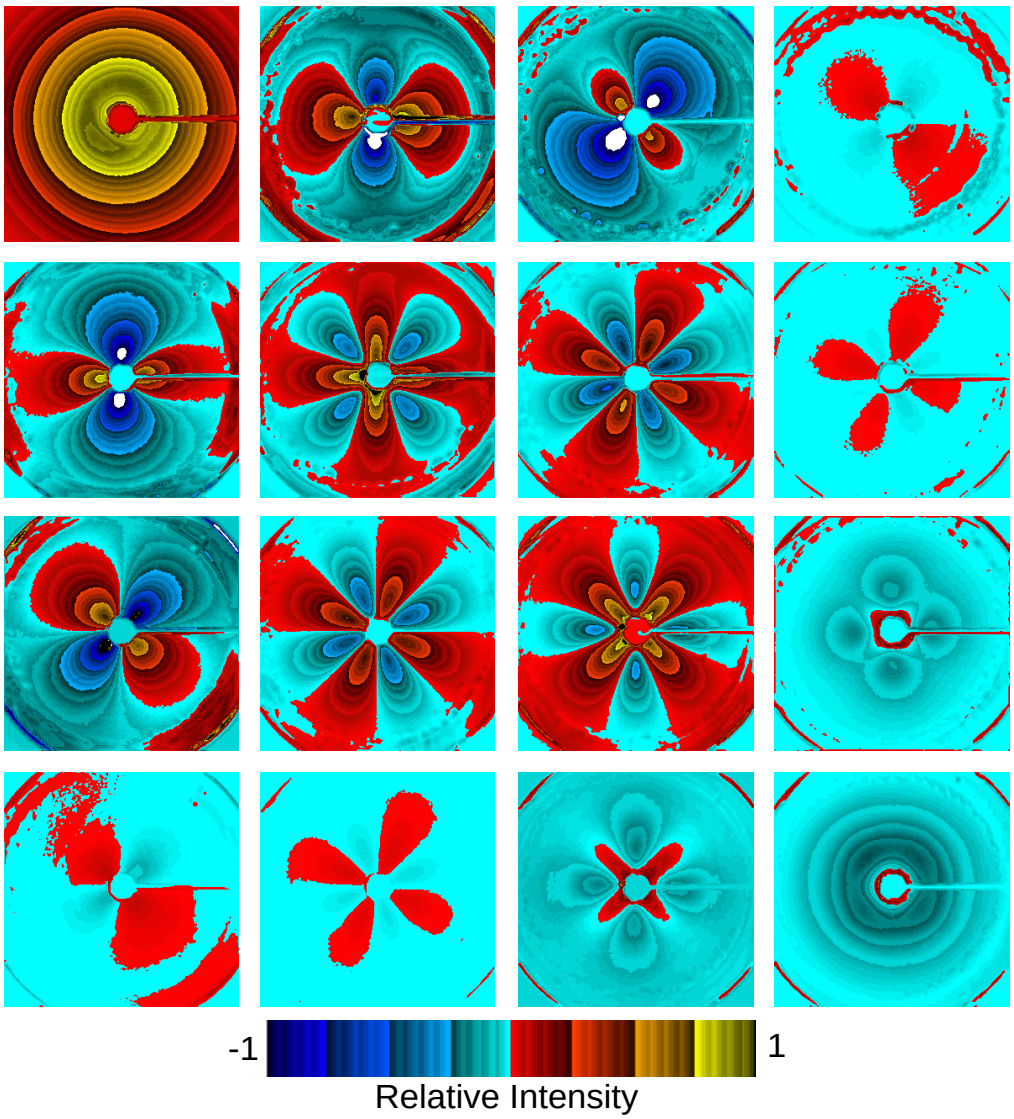

Fig.9. Diffuse-backscattering Mueller matrix of cancerous MR1 cell suspension with 10^8 cells/cm^3.

and μ_s' = 2.1 cm^{-1} (±10%) for the MR1 and M1 cells, respectively. The two matrixes are almost identical. Small differences can be observed for the M_{22} and M_{33} elements. In these matrix elements the negative values close to the center appear slightly more pronounced. Larger differences between the tumorigenic MR1 cells and the nontumorigenic M1 cells can be seen in the M_{44} elements.

The M_{44} element is radially symmetric for the MR1 cells as well as the M1 cells. Figure 10 shows the radial dependence along the y-axes of M_{44} for r = 0.4 to 1.6 mfp' (mfp' = transport mean free path = $1/\mu_s'$). The laser light enters the medium at r = 0 mfp'. Data for r < 0.4 mfp' is omitted because this range is covered or distorted by the optical mask. For radial distances r > 0.5 mfp' the M_{44} element for the MR1 suspension is smaller. This means that in this range the cancerous cell suspension flips the helicity of the incident light more than the noncancerous cell suspension.

Comparing Fig. 10 with the results found for polystyrene-sphere suspensions in Fig. 7, it is interesting to note that for distances larger than 0.9 mfp' from the light input point,

#2826 - $10.00 US
Received October 8, 1997; Revised December 2, 1997

backscattering from the cell suspensions is similar to backscattering from 497-nm-sphere suspension. However, for smaller distances the value of the M_{44} element for the polystyrene-sphere suspension decreases as the light incident point is approached, while the value of M_{44} for the cell suspensions increases. The reason for this behavior is unclear and further studies will be necessary. Possible explanations may be related to the nonspherical shapes of the scatterers within the cell, scattering contributions from particles with various sizes, or optical activity of the medium.

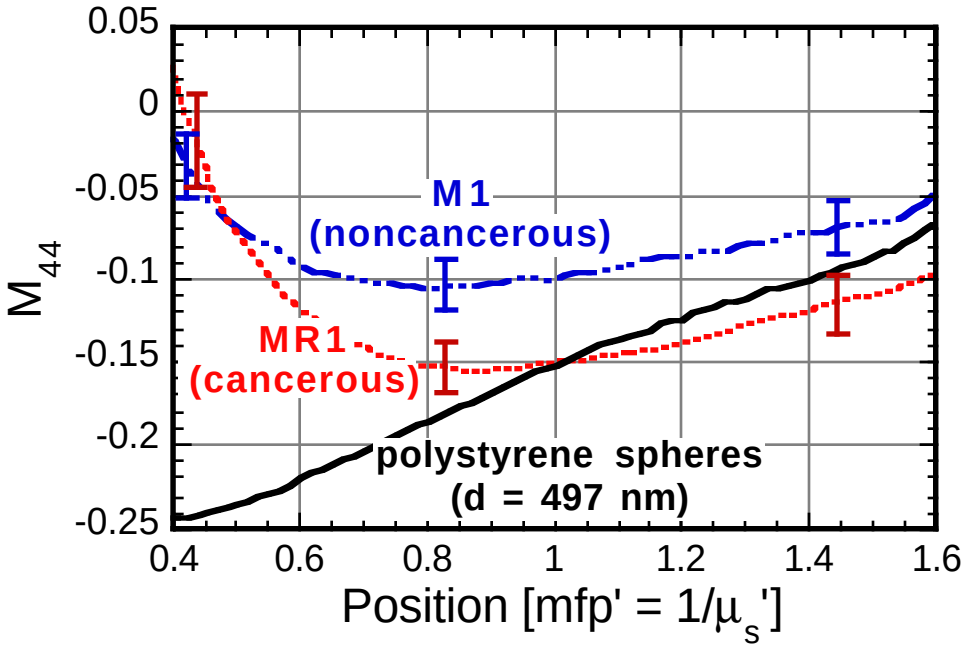

Fig. 10. Radial dependence of M_{44} obtained from cell suspensions . As a reference the result for a 497-nm-polystyrene-sphere suspension is also shown (see Fig.7).

4. Summary and conclusion

In this work we present a method and general framework for the study of diffusely backscattered polarized light from highly scattering media. Our method is an extension of the well known techniques of spatially resolved reflectometry and video reflectometry. These methods use unpolarized light in the study of optical properties (μ_s' and μ_a) of turbid media. We show that with the use of a polarized incident beam and the analysis of various polarization components in the diffusely backscattered light, complex, 2-dimensional, spatially varying surface-intensity patterns can be observed. These patterns can be used to gain additional information about the scattering medium and to distinguish between media with the same μ_s' and μ_a.

An infinite number of different backscattering measurements using polarized light can be performed by varying the polarization state of the incident beam and detecting different polarization components of the diffusely backscattered light. However, by introducing the Stokes-vector, Mueller-matrix concept for diffusely backscattered light, we provide a framework to select subsets of measurements that comprehensively describe the optical properties of backscattering media. With 49 measurements all 16 elements of the diffuse backscattering Mueller matrix can be determined. Knowing all 16 elements of this matrix one can calculate the polarization state of the backscattered light given any polarization state of the incident light. Therefore, knowing all 16 elements completely describes the medium in terms of optical properties.

#2826 - $10.00 US
Received October 8, 1997; Revised December 2, 1997

To illustrate the potential of the Mueller-matrix approach we studied polystyrene-sphere and biological-cell suspensions. Clear differences among different monodisperse polystyrene-sphere suspensions can be found in several matrix elements, even when the suspensions have the same scattering and absorption coefficients. We have shown that the M_{44} element, which is obtained from measurements employing right and left-hand polarized light, is especially sensitive to particle sizes in the suspension. Furthermore we have shown that suspensions of cancerous and noncancerous rat fibroblast cells can be best differentiated by the M_{44} element.

Further studies are necessary to fully explore the Mueller-matrix approach to analyzing diffusely backscattered light and it's possible use in biomedical diagnostics. For example, obtaining the full matrix for particle suspensions with various well-known size distributions may help understanding the patterns observed from cell suspensions. In contrast to suspensions, tissues are highly structured and often have preferred optical axes. These structures should affect the elements of the Mueller matrix. Furthermore, tissues have, in general, a higher scattering coefficient than the suspensions described in this study. This means that polarization effects will be limited to a smaller distance from the laser incident point. This may require the use of a microscope or fiber optics to spatially resolve the patterns in the matrix elements. Finally, it is highly desirable to develop an analytical or numerical model to simulate and predict the type of results discussed in this study.

Acknowledgements

This work was supported in part by grants CA71898 and ES07845 from the National Institutes of Health, a Postdoctoral Fellowship from the Director's Office at Los Alamos National Laboratory (LANL), the Laboratory Directed Research and Development Program at LANL, and funds from the Science and Engineering Research Semester (SERS) program operated by the Department of Energy.

#2826 - $10.00 US Received October 8, 1997; Revised December 2, 1997